

Paper

Plasma density and temperature evolution following the H-mode transition at JET and implications for ITER

The build-up of plasma parameters following the H-mode transition in JET has been analysed in view of its consequences for the alpha power evolution in the access to burning plasma conditions in ITER. JET experiments show that the build-up of plasma temperature both at the plasma core and the plasma edge occurs in timescales comparable to the energy confinement time. On the contrary, the evolution of the edge and core densities differs strongly depending on the level of plasma current in the discharge and of the associated NBI penetration. For higher plasma current H-mode discharges ($I_p > 2.0\text{-}2.5$ MA, depending on plasma shape), with naturally higher plasmas densities for which NBI penetration is poorer, the core density evolves in much longer timescales than the edge density leading to the formation of rather hollow density profiles. These hollow density profiles persist for timescales of several energy confinement times until they are usually terminated by a sawtooth. Modelling of the JET experiments with JETTO shows that the density build-up following the H-mode transition can be described with a purely diffusive model, despite the low collisionalities of high current H-mode plasmas at JET. The consequences of these JET experimental/modelling findings for the access to burning plasma conditions in the ITER QDT = 10 scenario are presented. Manuscript to be submitted to Nuclear Fusion

<i>Approval Process</i>			
	<i>Name</i>	<i>Action</i>	<i>Affiliation</i>
<i>Author</i>	Loarte A.	08-Mar-2013:signed	IO/DG/DIP/POP/SD/CMS
<i>Co-Authors</i>			
<i>Reviewers</i>	Campbell D.	01-Apr-2013:recommended	IO/DG/DIP/POP
<i>Approver</i>	Parravicini D.	02-Apr-2013:approved	IO/DG/ADM/GEA/DOC
<i>Document Security: level 1 (IO unclassified)</i>			
<i>RO: Das Saroj</i>			
<i>Read Access</i>	AD: ITER, AD: External Collaborators, AD: Section - Document Control, project administrator, RO		

Plasma density and temperature evolution following the H-mode transition at JET and implications for ITER

A. Loarte¹, M.J. Leyland², J.A. Mier³, M.N.A. Beurskens⁴, I. Nunes⁵, V. Parail⁴, P.J. Lomas⁴, G. R. Saibene⁶, R.I.A. Sartori⁶, L. Frassinetti⁷ and JET EFDA Contributors*

JET-EFDA, Culham Science Centre, Abingdon, OX14 3DB, UK

¹ITER Organization, Route de Vinon sur Verdon, 13115 Saint Paul Lez Durance, France

²Department of Physics, University of York, Heslington, York, YO10 5DD, UK

³Departamento de Física Aplicada, Universidad de Cantabria, 39005 Santander, Spain

⁴EURATOM/CCFE Fusion Association, Culham Science Centre, Abingdon OX14 3DB, UK

⁵Instituto de Plasmas e Fusão Nuclear, Av. Rovisco Pais, 1049-001 Lisboa, Portugal

⁶Fusion for Energy, C/ Josep Pla nº 2, 08019 Barcelona, Spain

⁷Association EURATOM-VR, Fusion Plasma Physics, EES, KTH, 10044 Stockholm, Sweden

Abstract : The build-up of plasma parameters following the H-mode transition in JET has been analysed in view of its consequences for the alpha power evolution in the access to burning plasma conditions in ITER. JET experiments show that the build-up of plasma temperature both at the plasma core and the plasma edge occurs in timescales comparable to the energy confinement time. On the contrary, the evolution of the edge and core densities differs strongly depending on the level of plasma current in the discharge and of the associated NBI penetration. For higher plasma current H-mode discharges ($I_p > 2.0\text{-}2.5$ MA, depending on plasma shape), with naturally higher plasmas densities for which NBI penetration is poorer, the core density evolves in much longer timescales than the edge density leading to the formation of rather hollow density profiles. These hollow density profiles persist for timescales of several energy confinement times until they are usually terminated by a sawtooth. Modelling of the JET experiments with JETTO shows that the density build-up following the H-mode transition can be described with a purely diffusive model, despite the low collisionalities of high current H-mode plasmas at JET. The consequences of these JET experimental/modelling findings for the access to burning plasma conditions in the ITER $Q_{DT} = 10$ scenario are presented.

E-mail contact of main author: alberto.loarte@iter.org

1. Introduction

Understanding of the physics mechanisms that determine plasma fuelling and core particle transport is required to predict both the plasma density profiles and fuelling requirements for burning plasmas in next step devices [Pacher 2008] as well as the access to burning plasma conditions and its possible control requirements. The evolution of the plasma density following the H-mode transition is particularly relevant for ITER because ITER high Q_{DT} plasmas are expected to operate at a relatively low margin above the H-mode threshold [Hawryluk 2009] and with a large contribution of the alpha heating to the total plasma heating power,

* See the Appendix of F. Romanelli et al., Proceedings of the 24th IAEA Fusion Energy Conference 2012, San Diego, USA.

$$P_{\alpha} = Q_{DT}/5 \times P_{add} \quad (1)$$

where P_{α} is the alpha heating, Q_{DT} is the fusion gain and P_{add} is the additional heating power. For $Q_{DT} \sim 5$ (long pulse high fusion yield ITER operation target) $P_{\alpha} = P_{add}$, and for $Q_{DT} \sim 10$ (inductive ITER operation with high Q_{DT}) $P_{\alpha} = 2 P_{add}$ [Hawryluk 2009] so that P_{α} constitutes a major contributor to the plasma heating power and the edge power flow. The alpha heating power itself is determined by the plasma density and temperature profiles. Therefore changes to the plasma parameters caused by confinement transitions, such as the L-H or the H-L transitions, affect the alpha heating evolution which in turn affects the edge power flow and thus the confinement state of the plasma. The complex interlink between the evolution of the edge power flow and the plasma parameters and the edge power flow in ITER is shown in a schematic form for the phase following the H-mode transition in a 15 MA $Q_{DT} = 10$ ITER plasma in Fig.1.a. Assuming that the build-up of the plasma energy from L-mode in ITER takes place in $\sim 3 \tau_E$ (energy confinement times of the full developed H-mode plasma conditions, see section 4 for further justification of this assumption) one can evaluate how the edge power flow would evolve for various assumptions of the plasma average density evolution. Fig.1.a illustrates a case in which the average density build up time scale is similar to that of the plasma energy. In this case, the plasma temperature increases after the L-H transition together with the density ensuring an increasing level of alpha heating which is sufficient to maintain an edge power flow (P_{loss}) at or slightly above the power required to sustain the H-mode confinement (P_{L-H}),

$$P_{loss} = P_{\alpha} + P_{add} - P_{rad}^{core} - dW_{plasma}/dt \geq P_{L-H} \quad (2)$$

where P_{rad}^{core} is the core plasma radiation and W_{plasma} is the plasma energy. Fig.1.b illustrates a case in which the average plasma density is assumed to increase in a much shorter time scale ($\sim \tau_E$) than that of the plasma energy ($\sim 3\tau_E$). In this case the plasma temperature remains unchanged by the H-mode transition and can even slightly decrease. Because of the large increase in P_{L-H} and in P_{rad}^{core} associated with the density rise, the edge power flow during the whole period after the H-mode transition to the burning plasma conditions remains under that required to sustain the H-mode (P_{L-H}) by a significant factor (more than ~ 2 times lower during the initial H-mode phase). Although it is commonly seen that H-modes can be sustained in their initial phase with an edge power flow lower than that required to access the H-mode regime in stationary phases, extended periods in time in such conditions usually lead to the loss of the high quality H-mode confinement [Sartori 2004]. Therefore it is likely that, in practice, the burning plasma conditions would not be accessible for the case illustrated in Fig.1.b and a return to L-mode conditions would be experienced by the plasma. In addition even if H-mode confinement is sustained, if the temperature decrease after the H-mode transition is significant, this could decrease the alpha heating power production during this phase. This is due to the stronger dependence (stronger than $\sim T^2$) of the DT reaction rate ($\langle \sigma v \rangle_{DT}$) for lower temperatures so that this decreases cannot be compensated by the density increase in this phase ($P_{\alpha} \sim n^2 \langle \sigma v \rangle_{DT}$). This effect, which is not taken into account to derive the schematic diagrams in Figs. 1.a and 1.b could further exacerbate the problem of the low edge power flow to sustain the H-mode during the initial phase in the case illustrated in Fig. 1.b.

Obviously, no quantitative conclusions regarding the behaviour of real ITER plasmas can be derived from these schematic diagrams, which are derived under very simplistic approximations (i.e. fixed density and temperature shape, etc.). They are nevertheless useful to identify the specific issues that are of concern regarding the access to burning plasma conditions

in ITER. As identified in Figs.1.a and 1.b a key issue to understand the access to burning plasma conditions in ITER is the behaviour of the plasma density and temperature as they (in particular their evolution in the central part of the plasma) influence the evolution of the alpha heating power as well as (for the density) the power required to sustain the H-mode confinement. Of particular importance for ITER is thus to understand the physics processes that determine the core temperature and density evolution following the H-mode transition in conditions of low core particle source and low plasma collisionality :

a) A low core fuelling is expected in ITER as the only heating method in ITER that causes a source in the core plasma is the Negative Neutral Beam Injection (NNBI) and pellet injection in ITER only leads to peripheral fuelling due to the high (multi-keV) edge temperatures [Garzotti 2012]. Because of the high energy of the beams required to deposit power in the ITER central plasma region (~ 1 MeV) [Wagner 2010], the particle source associated with NBI heating in ITER is much smaller than in present experiments. Typically the core fuelling of ITER plasmas by NNBI is one order of magnitude smaller than in present experiments while the plasma particle content is one to orders of magnitude larger.

b) Plasma collisionality is found to be a good ordering parameter in H-mode experiments to quantify the degree to which stationary density profiles will be peaked [Angioni 2007a, Beurskens 2013] and thus for the relative magnitude of the relation between turbulent inwards and outwards particle fluxes associated with the expected level of TEM and ITG turbulence in ITER [Angioni 2009].

To understand the physics processes dominating the density and temperature following the L-H transition in ITER, high current H-mode experiments ($I_p \geq 3.0$ MA) are particularly interesting. Because of the high I_p and the empirical relation between the plasma current and plasma density in H-modes, the plasma density of these plasmas in JET is high and comparable to that of ITER plasmas ($\sim 1.0 \cdot 10^{20} \text{ m}^{-3}$) while the plasma temperature remains high ($T_{e,i}(0) \sim 5$ keV) [Nunes 2010] and the core plasma collisionality relatively low. In these conditions, the JET NBI particle deposition profiles are very hollow so that the effective core fuelling of these plasmas resembles qualitatively that expected in ITER, i.e. a large peripheral fuelling in the edge of the main plasma (neutral gas fuelling and NBI in JET versus pellet fuelling in ITER) [Garzotti 2012] with very low core fuelling.

This paper reports on the analysis of the density and temperature evolution following the L-H transition in a set of H-mode experiments at JET, which span a range of plasma currents up to $I_p = 4.3$ MA [Nunes 2010], and draws conclusions regarding the expected plasma behaviour in ITER. Section 2 provides an overview of the experimental results, describes the analysis techniques used and the key results obtained for the plasma and temperature evolution following the L-H transition. Section 3 describes the modelling of the JET experimental results. Section 4 describes the application of the same models, with the modelling assumptions found to be suitable to describe the JET experiments, to ITER. Finally, section 5 summarises the results and draws conclusions. In this paper we will not deal with the important issue of the plasma behaviour during and following the H-L transition. This is presently subject of experimental and modelling studies and will be the subject of a follow-up paper.

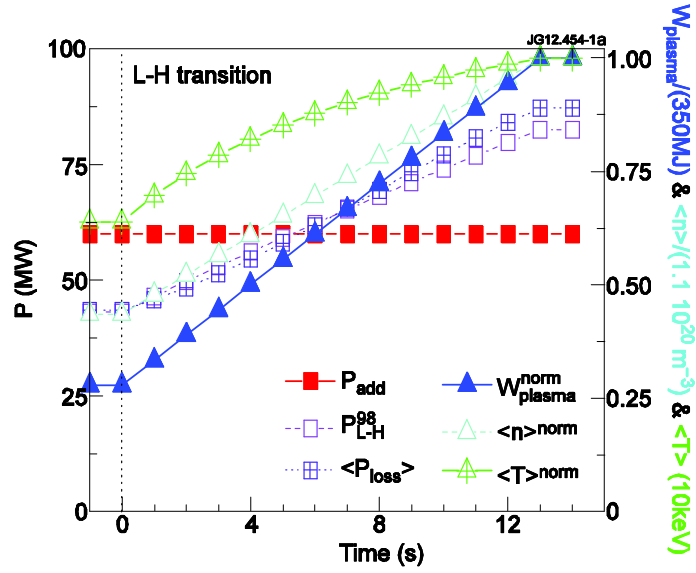


Fig.1.a. Schematic representation of the evolution of the plasma energy, average plasma density and temperature, heating power and edge power flow in ITER 15 MA $Q_{DT}=10$ plasmas following the L-H transition. In this figure the average plasma density is assumed to increase from its L-mode to its stationary H-mode value in 12 s ($\sim (3-4) \tau_E$). For comparison, the evolution of the edge power flow required to sustain the H-mode confinement (P_{L-H} from the ITER scaling law [Martin 2008]) is shown.

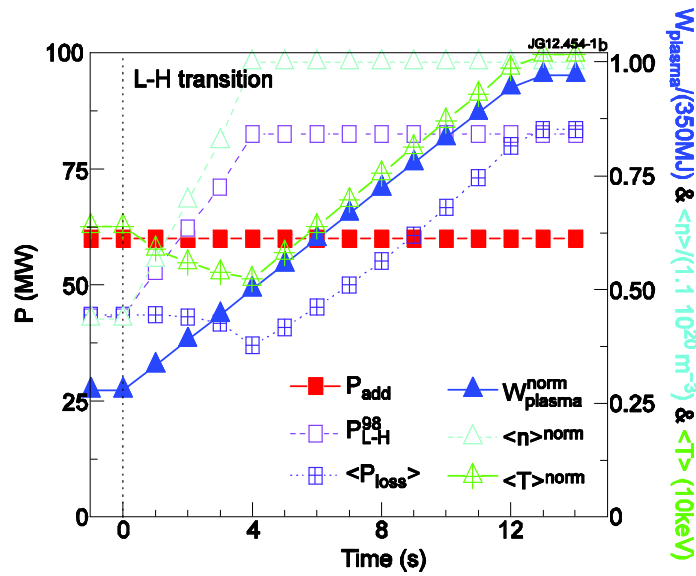


Fig.1.b. Schematic representation of the evolution of the plasma energy, average plasma density and temperature, heating power and edge power flow in ITER 15 MA $Q_{DT}=10$ plasmas following the L-H transition. In this figure the average plasma density is assumed to increase from its L-mode to its stationary H-mode value in 4 s ($\sim \tau_E$). For comparison, the evolution of the edge power flow required to sustain the H-mode confinement (P_{L-H} from the ITER scaling law [Martin 2008]) is shown.

2. Edge and core plasma parameters build-up from L-mode to stationary ELMy H-mode in JET experiments

In order to characterise the physics processes that determine the plasma temperature and density build-up and their timescales after the H-mode transition, a set of JET H-mode discharges has been analysed. They comprise H-mode discharges with a range of plasma currents (I_p) from 1.0 MA to 4.3 MA, low and high plasma triangularity (δ), with dominant NBI heating and fuelling by gas puffing with carbon plasma facing components [Nunes 2010]. A typical example of the evolution of the plasma parameters following the H-mode transition in a high current H-mode at JET is shown in Fig. 2. As can be seen in this figure, the largest and fastest changes in plasma density and temperature after the L-H transition occur near the plasma edge. This is caused by the formation of the edge transport barrier which builds up in timescales similar to the energy confinement time (τ_E) in the stationary phase of the discharge. Of particular interest, in relation to the ITER issues discussed in the introduction, is the fact that the core plasma density after the H-mode transition increases over a much longer period ($4-5 \tau_E$) with the core temperature increasing weakly from its value in L-mode in this phase. The different timescales for edge and core density build-up lead to the transient formation of considerably hollow density profiles, which coexist with hollow NBI particle deposition profiles, as shown in Figs. 3.a-e. It is important to note that the hollow density profiles in Figs. 3.c & 3.d are seen both for ions and electrons and are thus determined by the transient evolution of the main ion density profiles from L-mode to stationary H-mode conditions. This is unlike other plasma conditions (such as long ELM-free H-modes) in which hollow density profiles in the edge region of the plasma have been previously measured for the electrons and not the main ions resulting from the accumulation of impurities at the plasma edge due to the lack of ELMs (which expel impurities) in these conditions [Scotti 2012].

In most JET high current H-modes the hollowness of the density profile decreases in time as the H-mode progresses until it is terminated suddenly by a sawtooth that flattens the density profiles, as shown in Fig.3. The duration of the phase with hollow density profiles and the magnitude of the density de-peaking has been characterised by analysing the ratio of the edge density ($\rho = r/a = 0.8$) to the core density ($\rho = r/a = 0.2$) and fitting it by a Gaussian profile in time as shown in Fig. 4. The choice of these two particular radii is determined by diagnostic issues (the innermost measurement of the electron density and temperature profiles with the required time resolution by the High Resolution Thomson scattering in JET is $\rho = 0.2$ for these discharges) and ELM physics issues (points with $\rho > 0.8$ are strongly affected by the modulation of the ELMs at JET [Loarte 2002, Beurskens 2009]). The same methodology can be applied to the temperature profiles but, as already shown in Fig. 3 and more in detail in Fig. 4, the temperature profiles react rather stiffly to the L-H transition and the core and the edge temperatures increase in the same proportion so that no large change of this ratio in the initial phase after the H-mode transition is seen experimentally. The results of the analysis of the magnitude of the density hollowness (defined as $n_e(\rho=0.8)/n_e(\rho=0.2)$) and the duration of the hollow density profiles can be found in Fig. 5. As shown in Fig. 5, the magnitude and duration of the hollow phase of the density profiles increases, to first order, with plasma current of the H-mode discharge. The scatter in these figures is due to the fact that, in some cases, the density evolution is affected by the occurrence of the first sawtooth after the H-mode transition, thus not allowing the particle-transport driven natural relaxation of the density profiles to occur.

JET Pulse No: 79676:

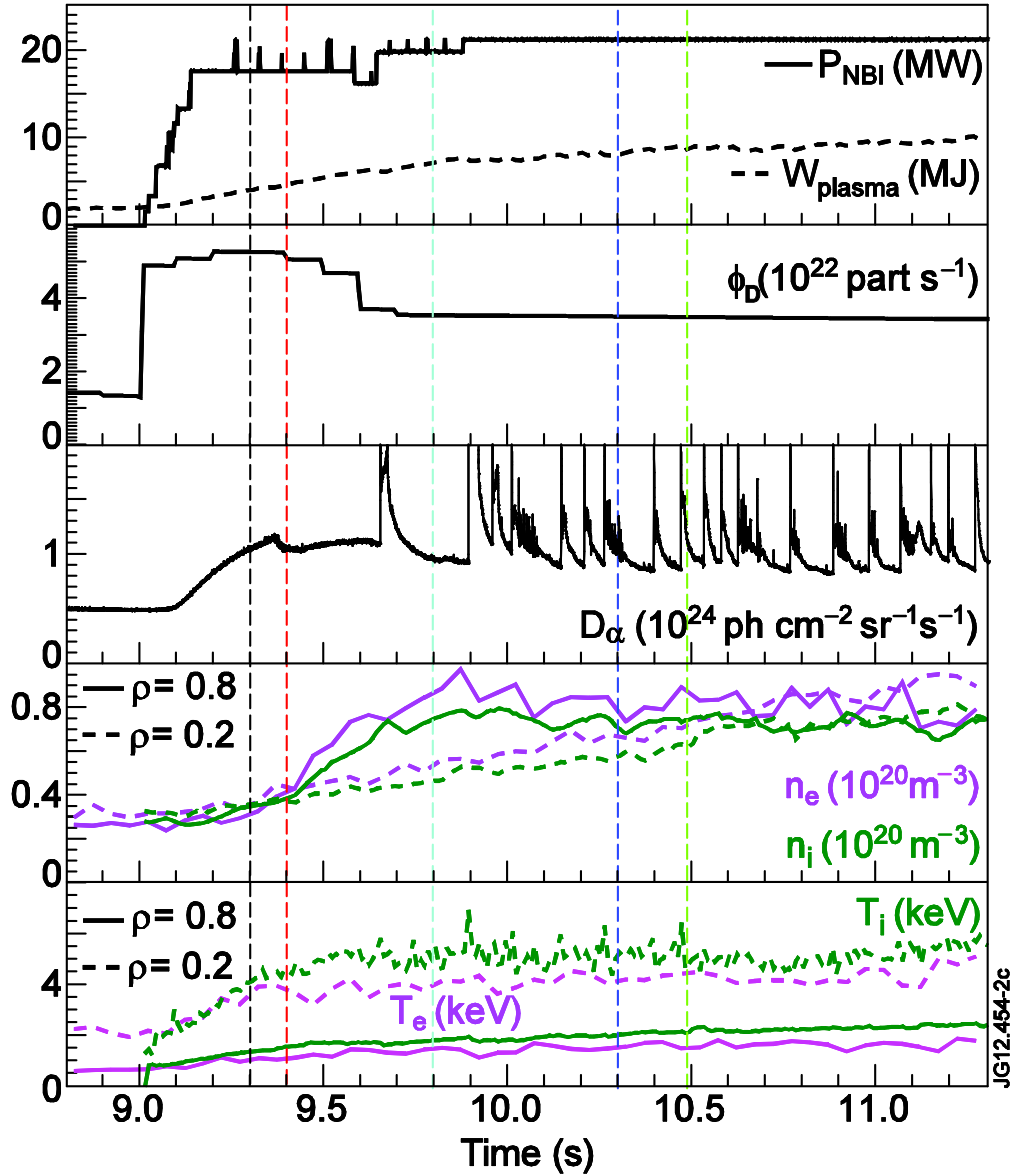
4.3 MA/3.4T, $P_{\text{NBI}} = 21\text{MW}$, $\tau_E = 0.4\text{s}$ 

Fig.2. Additional heating power by NBI (P_{NBI}), plasma energy (W_{plasma}), gas fuelling rate(ϕ_D), D_α emission from the divertor and evolution of the core ($\rho = 0.2$) and edge ($\rho = 0.8$) electron and ion density and temperature following the L-H transition in a JET high current H-mode.

The formation of hollow density profiles is correlated with the formation of hollow NBI particle deposition profiles. Hollow NBI particle deposition profiles are found to develop at lower levels of plasma current for higher triangularity plasmas than for the lower triangularity ones as shown in Fig. 6.a. As such, the triangularity is not the main parameter that controls the formation of hollow NBI particle deposition profiles but the higher edge densities that are accessible with higher triangularity configurations, as shown by the comparison between Fig. 6.a and Fig.6.b.

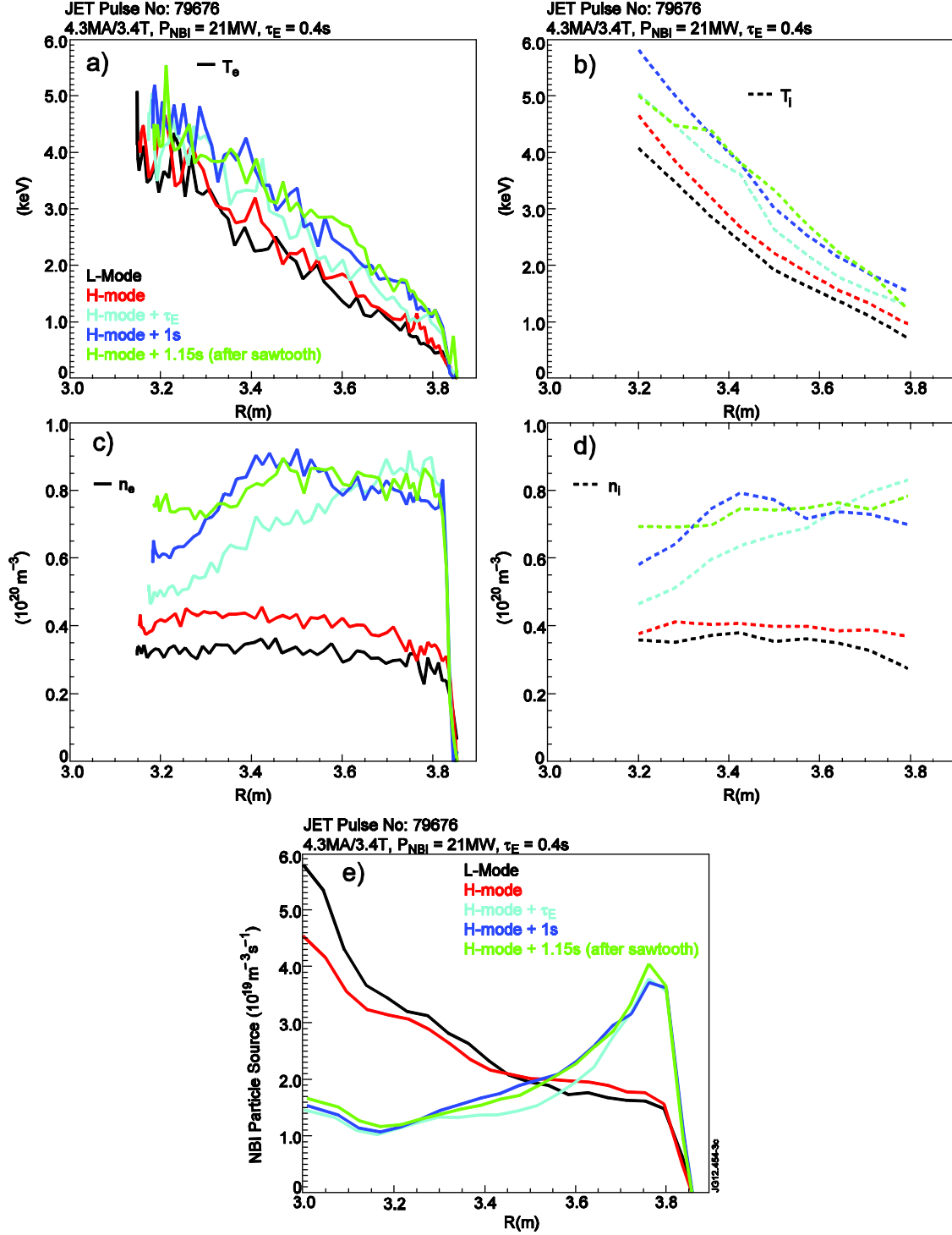


Figure 3. a) Electron and b) ion temperatures, c) electron and d) ion densities and e) NBI particle deposition profiles versus major radius (R) at five times in the evolution of the JET high current discharge in Fig. 2. The profiles span the range in time from L-mode to the first sawtooth in the stationary phase of the H-mode phase and show the formation of hollow ion and electron density profiles and their evolution in time up to their termination by a sawtooth. During the hollow density profile phase, the NBI particle deposition profiles are also hollow.

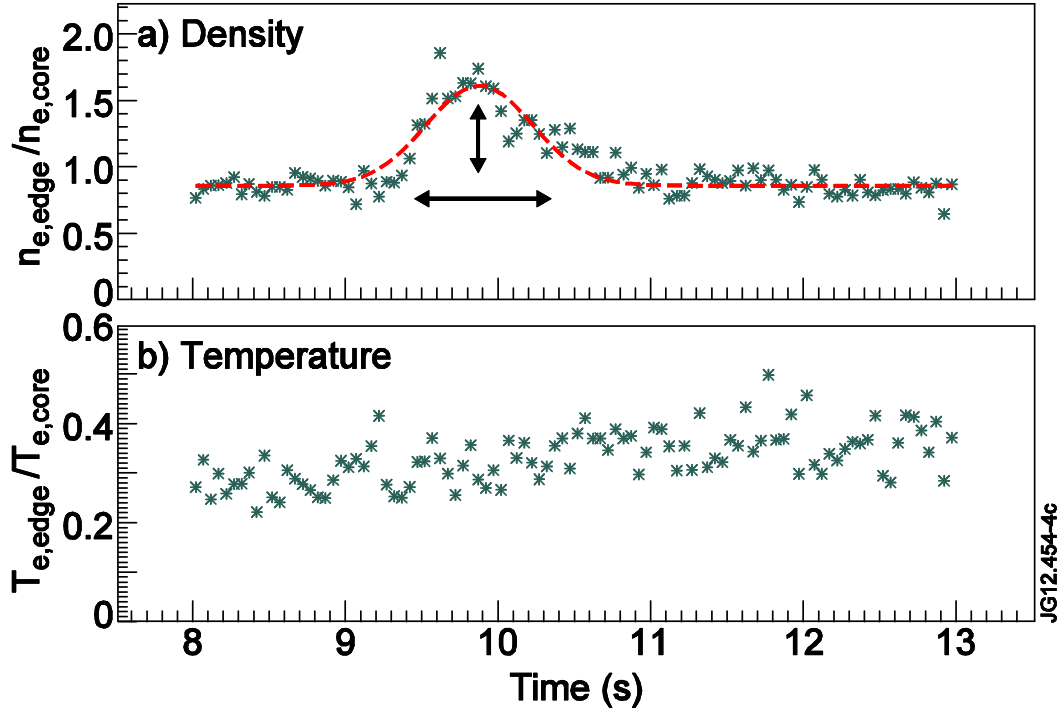


Figure 4. a) Ratio of the electron density at the edge ($\rho = 0.8$) to the core density ($\rho = 0.2$) showing the formation of a hollow density profile which lasts for a period of about 0.8 seconds for a JET high current H-mode. b) Ratio of the electron temperature at the edge ($\rho = 0.8$) versus the core temperature ($\rho = 0.2$) for the same discharge as in a), showing the lack of change of this ratio when the plasma enters the H-mode, unlike the density profiles.

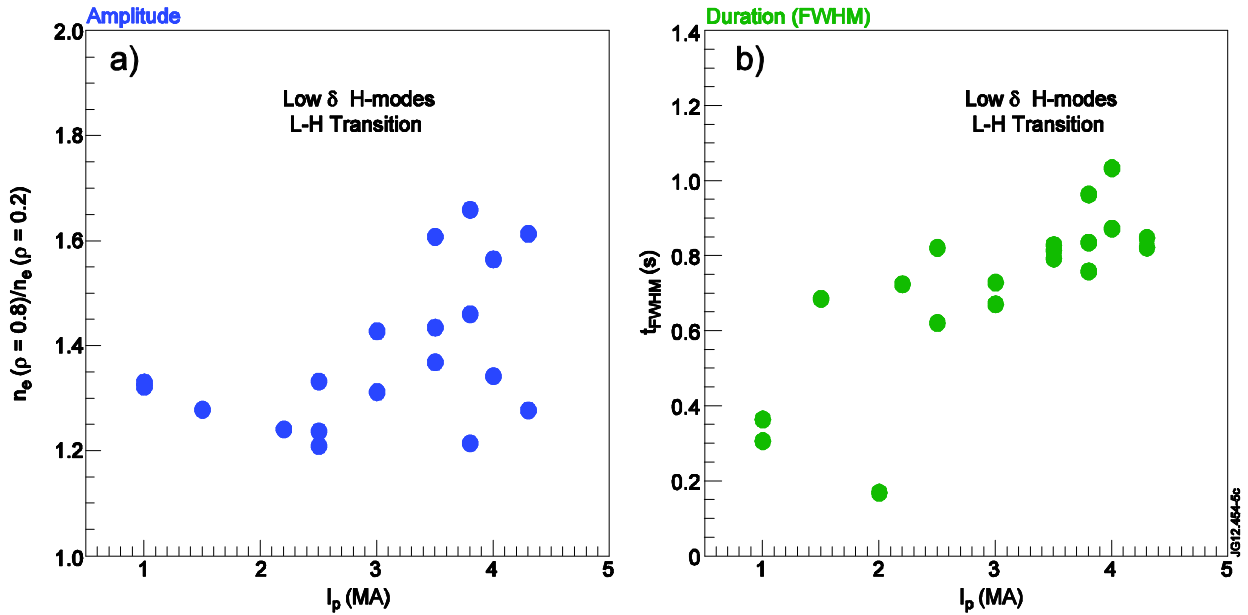


Figure 5. a) Maximum value of the ratio of the electron density at the edge ($\rho = 0.8$) to the core density ($\rho = 0.2$) versus plasma current for JET H-modes. b) Duration of the phase with hollow density profiles versus plasma current for JET H-modes.

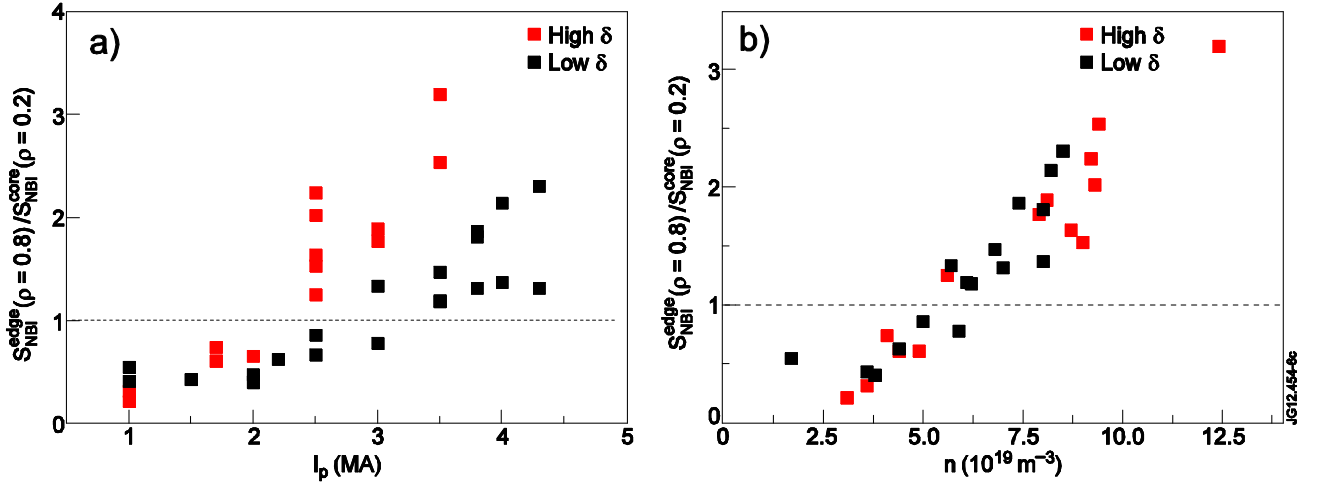


Figure 6. a) Ratio of the NBI particle source at the edge ($\rho = 0.8$) and at the core ($\rho = 0.2$) versus plasma current for high and low δ discharges. b) Ratio of the NBI particle source at the edge ($\rho = 0.8$) and at the core ($\rho = 0.2$) versus edge plasma density ($\rho = 0.8$) for high and low δ discharges.

As described in the introduction, for predicting the build-up of the alpha power in ITER it is important to understand the timescale over which edge and core densities and temperatures increase following the H-mode transition. These timescales have been characterised for the JET set of H-mode discharges considered in this paper by applying two analysis techniques : fitting the density and temperature evolution at two representative radii in the profile (namely $\rho = 0.2$ and 0.8) by a modified hyperbolic tangent fit but in time instead of space [Groebner 2001] or by a linear fit. The application of these fits is shown in Fig. 7 for the electron density and temperature and produces similar results. The results of the analysis by applying the hyperbolic tangent fit method for JET low triangularity H-modes are shown in Fig. 8.a and 8.b for both the electron and ion temperatures and densities. As shown in these figures the edge and core ion and electron temperatures build up in similar timescales which are comparable to that of the energy confinement time in these experiments ($\tau_E \sim 0.3-0.4$ s). On the contrary, the timescales for edge and core ion and electron density evolution differ strongly from those at the edge and the difference depends on the level of plasma current. For the largest plasma currents the electron and ion core density build up over timescales that can reach up to $\sim 6 \tau_E$ for 4.3 MA. It should be noted that the weak variation of the energy confinement time with increasing current in these experiments is due to the fact that the additional heating power is increased approximately linearly with increasing $I_p \times B_t$, which aims at keeping a similar ratio of the injected power to the H-mode threshold power all levels of plasma currents [Nunes 2010]. This increase in additional power level compensates the expected increase of the energy confinement time with plasma current and density expected from H-mode energy confinement. Similar results are obtained for H-modes with higher triangularity, as shown in Fig. 9 for the electron density and temperature. The level of current at which long timescales (~ 1 s) for the core density evolution are observed seems to be somewhat lower (2.5 MA instead of 3 MA) for higher δ discharges, which is consistent with the higher plasmas densities achieved at high δ and the appearance of hollow NBI particle deposition profiles as shown in Fig. 6.

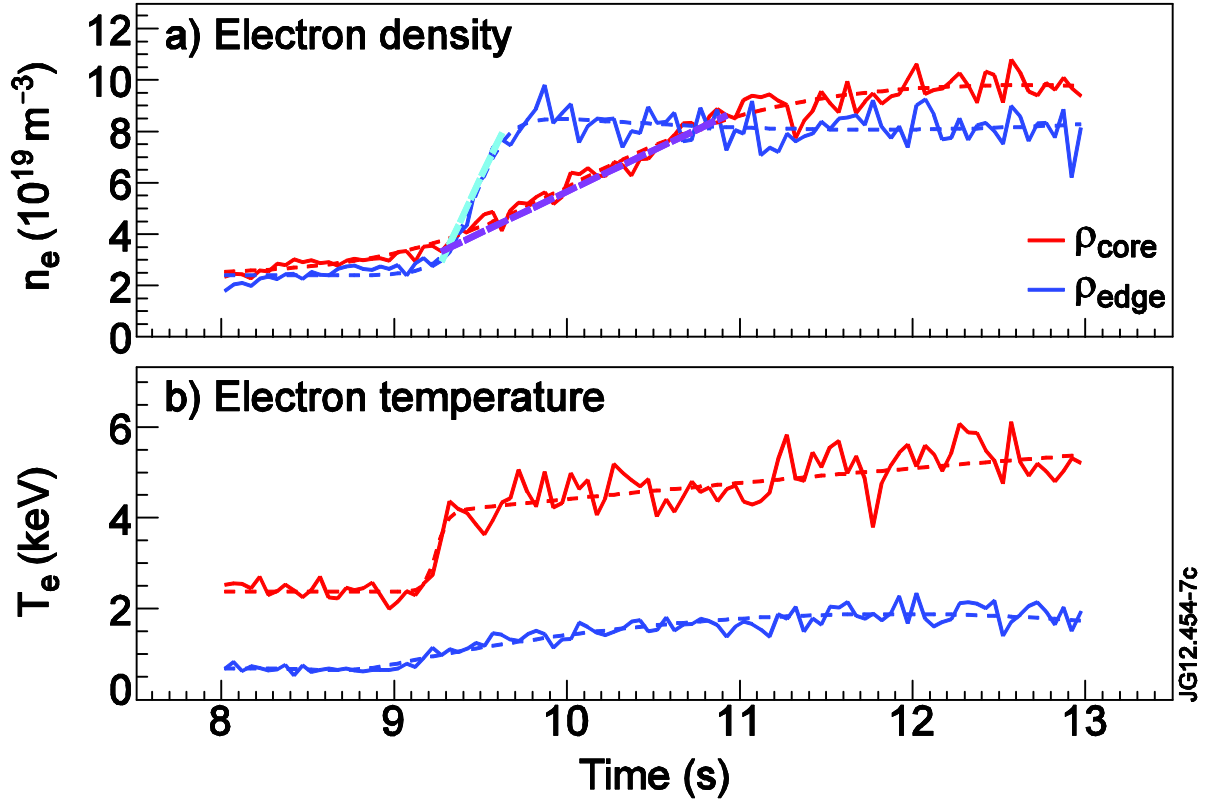


Figure 7. Evolution of the core ($\rho = 0.2$) and edge ($\rho = 0.8$) electron density (a) and temperature (b) following the H-mode transition in a 4.3 MA H-mode discharge at JET and the corresponding modified hyperbolic and linear fits utilized for the characterisation of their evolution timescale.

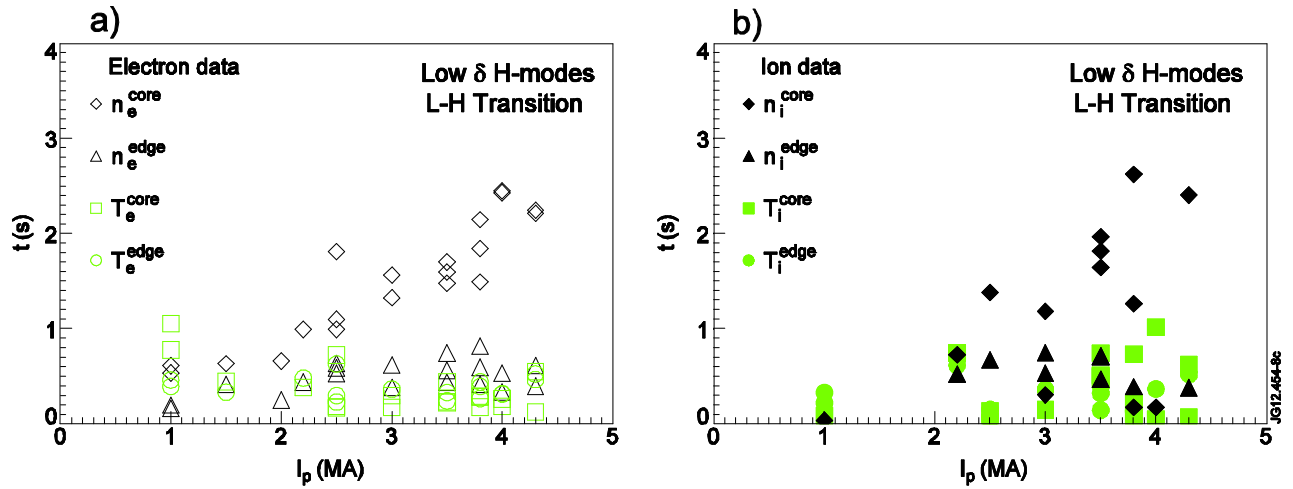


Figure 8.a) Timescale for core ($\rho = 0.2$) and edge ($\rho = 0.8$) electron temperature and density evolution following the H-mode transition in JET low δ discharges for a range of plasma currents. b) Timescale for core ($\rho = 0.2$) and edge ($\rho = 0.8$) ion temperature and density evolution following the H-mode transition in JET low δ discharges for a range of plasma currents.

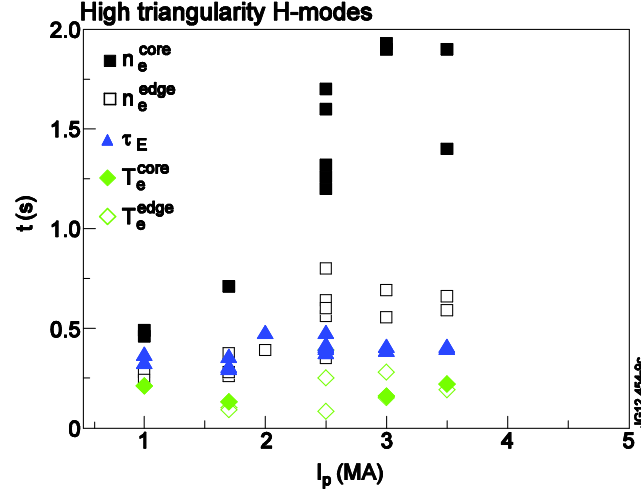


Figure 9. Timescale for core ($\rho = 0.2$) and edge ($\rho = 0.8$) electron temperature and density evolution following the H-mode transition in high δ JET H-modes for a range of plasma currents. The energy confinement time (τ_E) during the stationary phases of these discharges is shown for comparison.

The long timescales for the evolution of the core density cannot be attributed to a decrease of the central NBI particle source for higher I_p H-modes at JET. In fact, the formation of hollow NBI particle deposition profiles, associated with the higher plasma edge density in H-mode for higher I_p , compensates the increase in NBI power and total NBI particle flux in these experiments [Nunes 2010] ($\sim I_p \times B_t$ as discussed above) so that the core particle source from NBI is only weakly dependent on plasma current, as shown in Fig.10.

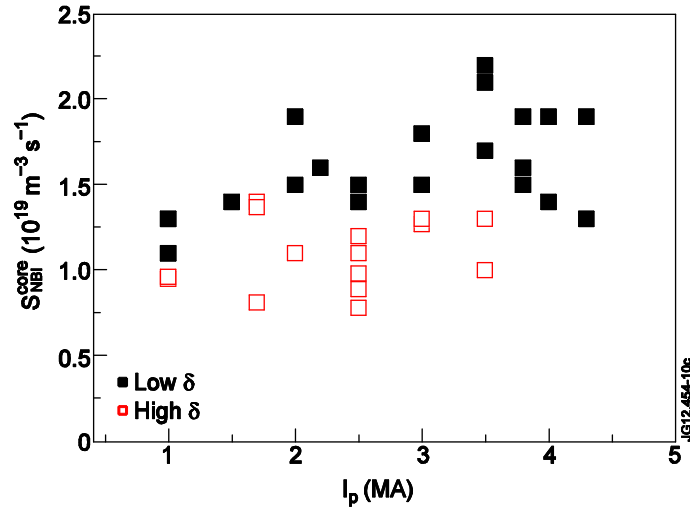


Figure 10. Average NBI particle source density in the central region of the plasma ($\rho \leq 0.2$) versus plasma current for low and high δ H-modes at JET. The high δ H-modes tend to have a lower core NBI particle source for a given value of the plasma current because of the higher densities and lower beam penetration which are achieved in high δ versus low δ H-modes. For both low and high δ H-modes there is not a marked decrease or increase of the magnitude of the core NBI source with plasma current.

3. Modelling of the H-mode density build-up in JET H-modes

Deriving implications of the observed density behaviour in JET low core particle source H-modes for ITER requires the application of appropriate modelling. These models should be first validated/compared against the JET experimental results and then applied to the specific ITER conditions (i.e. variable P_α due to varying density and temperature after the access to the H-mode). Therefore, the density build-up phase in these discharges has been modelled with JETTO, which includes an edge transport barrier model (modelled with $D_{e,i}$, $\chi_{e,i}$ values as given by ion neoclassical transport and no anomalous pinch), a model of the NBI particle source and from gas puffing. Core transport has been modelled with the Bohm/gyroBohm model for the particle and energy transport as described in [Garzotti 2003].

In the simulation of the JET discharges the level of edge particle source by gas puffing is adjusted to reproduce the experimental pedestal density behaviour. This is appropriate since the main aim of the studies is to understand the physics processes of core particle transport which do not require a full integrated modelling of the core and pedestal plasma together with SOL and divertor sources. For the modelling considered in this paper two assumptions have been used regarding the existence of an anomalous inwards pinch : $v_{\text{pinch}} = 0$ and $v_{\text{pinch}} = 0.5 D \rho/a$ (a positive inwards pinch velocity corresponds to a negative radial velocity). The value of $v_{\text{pinch}} = 0.5 D \rho/a$ is required to model the stationary density profiles in JET discharges over a range of parameters, particularly for L-mode conditions [Garzotti 2003] and is of a magnitude which is consistent with GLF23 predictions for the expected density peaking in ITER [Garzotti 2012].

Modelling assumptions to reproduce the core density build-up following the H-mode transition in JET has revealed two significant differences with respect to previous findings of stationary and sawtoothed H-modes :

a) Contrary to expectations from stationary density profile simulations, it is found that the slow rise of the core density build-up for conditions with low NBI core source, typical of high I_p H-mode discharges at JET, can only be accurately reproduced by assuming that there is no anomalous pinch during this phase ($v_{\text{pinch}} = 0$).

b) In addition, the slow core density rise requires a low value of D in the sawtooth-free core plasma region, typically $D = (0.25-0.5) D_{\text{BgB}}$, where D_{BgB} is the value of the Bohm/gyroBohm diffusion coefficient used for the stationary simulations of JET plasma density profiles [Garzotti 2003]. The diffusion coefficient required to model the transient density evolution in the outer half of the plasma is typically a factor 4-8 times larger than in the core.

The results for two simulations of high current H-modes are shown in Fig. 11.a and b. The main difference between these two discharges (besides a higher plasma current for the discharge in Fig.11.b) is the level of gas fuelling following the L-H transition. This level is low for the discharge 78703 (gas fuelling rate of $\sim 7 \cdot 10^{21} \text{ s}^{-1}$) and moderate/high (gas fuelling rate of $\sim 3.5 \cdot 10^{22} \text{ s}^{-1}$) for the discharge 79676.

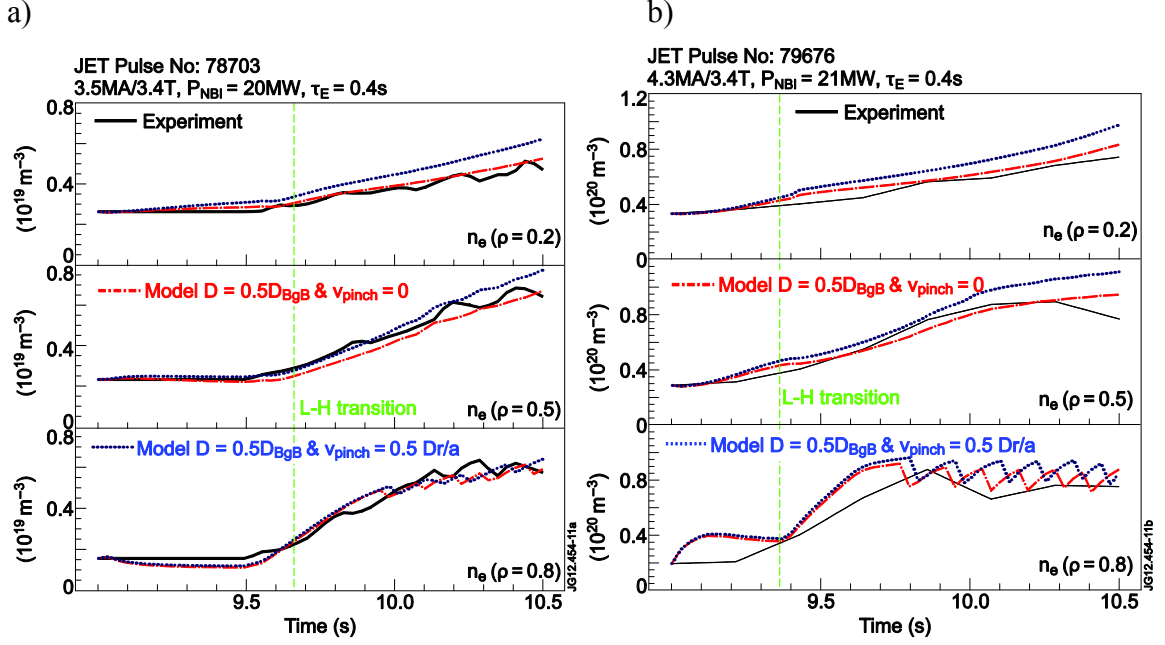


Figure 11. a) Measured and modelled electron density evolution at three radial positions from the central region to the edge (top to bottom $\rho = 0.2$, $\rho = 0.5$ and $\rho = 0.8$) for a high current H-mode discharge at JET with low gas fuelling rate (78703). b) Measured and modelled electron density evolution at three radial positions from the central region to the edge (top to bottom $\rho = 0.2$, $\rho = 0.5$ and $\rho = 0.8$) for a high current H-mode discharge at JET with medium/high gas fuelling rate (79676).

The values used for diffusion coefficients used in the modelling of the density evolution of a range of JET H-modes with $v_{\text{pinch}} = 0$ and various levels of plasma current are shown in Fig. 12. As mentioned above, these values are lower than those derived for stationary conditions and are very low in the plasma central region, which remains sawtooth-free during this phase. As expected from the Bohm/GyroBohm scaling, D decreases with increasing plasma current magnitude, which is consistent with the increased time scale for the evolution of the core density measured experimentally (see Figs. 8 and 9).

The physics mechanisms that lead to this very low level of particle transport in the transient phase of high current JET H-modes with low core NBI fuelling remains to be studied in detail. However, it is important to note that $T_e \sim T_i$ during this phase (due to the high plasma density of these discharges) and, because of the high current, the values of plasma temperature are moderately high so that the plasma collisionality is very low. In some cases, the plasma collisionality in the transient phase of these JET H-mode discharges can reach values similar to that of the ITER $Q_{\text{DT}} = 10$ stationary conditions, as shown in Fig. 13. For these low collisionalities a significant inwards pinch is expected from the empirical database for stationary H-mode conditions and present understanding of turbulent particle transport [Angioni 2007a, Beurskens 2013]. This is in contrast to what is deduced from the simulations of the transient density evolution discussed above which point towards a very low or zero pinch velocity in these JET H-mode conditions. The lack of a sizeable inwards pinch velocity in these low collisionality conditions at JET could be due to the negative scale length of the density profiles (hollow), as indicated by gyrokinetic modelling of JET H-modes that show a very low value of the inwards

anomalous particle flux for very flat density profiles (i.e. $v_{\text{pinch}} = 0$) [Angioni 2007b]. Further turbulent particle transport studies are in progress to evaluate if this argument can explain qualitatively the observed JET behaviour and what its implications for ITER would be.

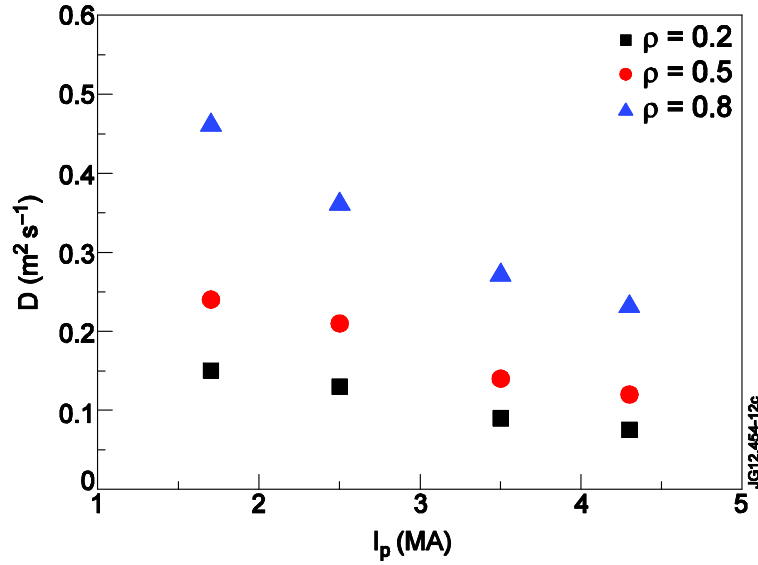


Figure 12. Values of the particle diffusion required to model the transient density behaviour after the H-mode transition in JET for three radial positions ($\rho = 0.2$, $\rho = 0.5$ and $\rho = 0.8$) versus plasma current.

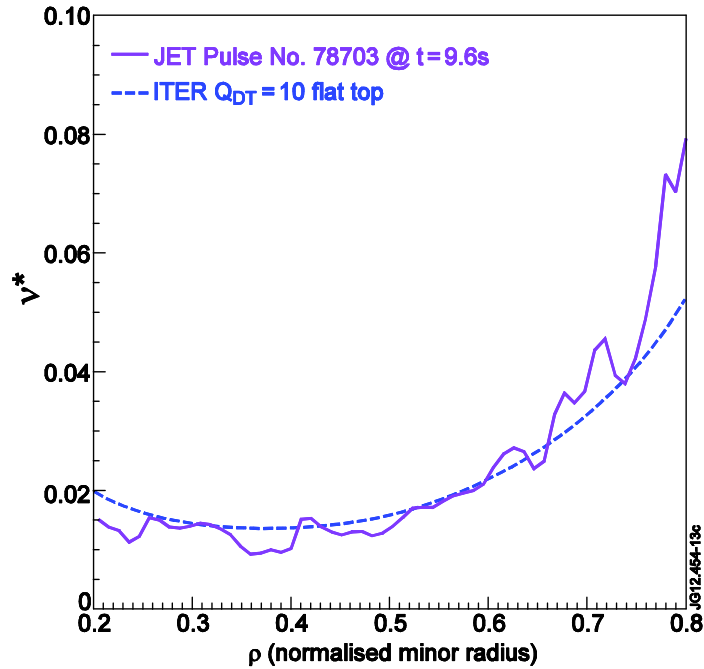


Figure 13. Plasma collisionality versus normalised minor radius for a time point in the middle of the density build up phase after the H-mode transition for a high current JET H-mode compared to that expected in the stationary phase of an ITER 15 MA $Q_{DT}=10$ plasma.

4. Modelling of access to $Q_{DT}=10$ burning plasma conditions in ITER

Modelling of the access to the full performance phase of ITER in the 15 MA scenario with $P_{\text{additional}} = 53$ MW has been carried out with the same transport assumptions which have been used to model the JET H-modes. In the ITER case, core plasma fuelling is provided by the negative NBI particle source and pellet fuelling. The negative NBI source in ITER is very small ($\leq 2 \cdot 10^{20} \text{ s}^{-1}$) due to the high energy of the injected neutrals (~ 1 MeV) while the pellet fuelling is limited by the total maximum pumping/throughput foreseen for ITER operation in the $Q_{DT} = 10$ scenario of $\sim 10^{23} \text{ s}^{-1}$ for 500s [Hawryluk 2009]. As shown in Fig. 14, for the two assumptions for particle transport used in these simulations (the same as used for modelling of the JET experiments), the evolution of the core plasma density is slow enough to allow the plasma temperature and fusion power to build up smoothly to full performance following the L-H transition. In agreement with the JET experimental findings, the plasma temperature both at the core and the edge build up in relatively short time scales which are comparable with $\sim \tau_E$. Most importantly, the core plasma temperature remains at all times at values above ~ 10 keV, range in which the DT reaction rate scales as $\sim T^2$, and thus with the square of the core plasma pressure, as shown in Fig. 15.a. The inclusion of an inwards particle pinch in this phase ($v_{\text{pinch}} = 0.5 D \rho/a$) leads to a higher core density and to lower core temperature as shown in Figs. 15.a and b. This extends somewhat (by $\sim \tau_E$) the duration of the period over which the edge power flow remains close to the power level required to sustain the H-mode (P_{L-H}), as shown in Fig. 14, and thus the phase during which a loss of the H-mode may occur in experiment. On the other hand, if the return to L-mode would not take place, the fusion performance of the plasma simulation including a pinch is much larger than that obtained for the plasma in which transport is purely diffusive. This is due to the stationary peaking of the density profiles when a pinch is included which, in these ITER simulations, lead to a peaking of the plasma pressure profiles.

It is important to note that, contrary to the high I_p JET H-modes, the access to burning plasma conditions in ITER will most likely be sawtooth free. Due to the stabilizing effects of fast particles (produced by the additional heating systems and the alpha particles themselves), the sawtooth period in ITER during the access to burn and the follow-up stationary $Q_{DT}=10$ phase is expected to be very long (~ 30 -40 s) [Hender 2007]. This is significantly longer than the expected time for the relaxation of the density profiles (10-20s, depending transport assumptions) in these simulations. Therefore, it is not likely that density profiles will be flattened by sawtooth activity before they achieve their stationary shape for burning plasma conditions in ITER.

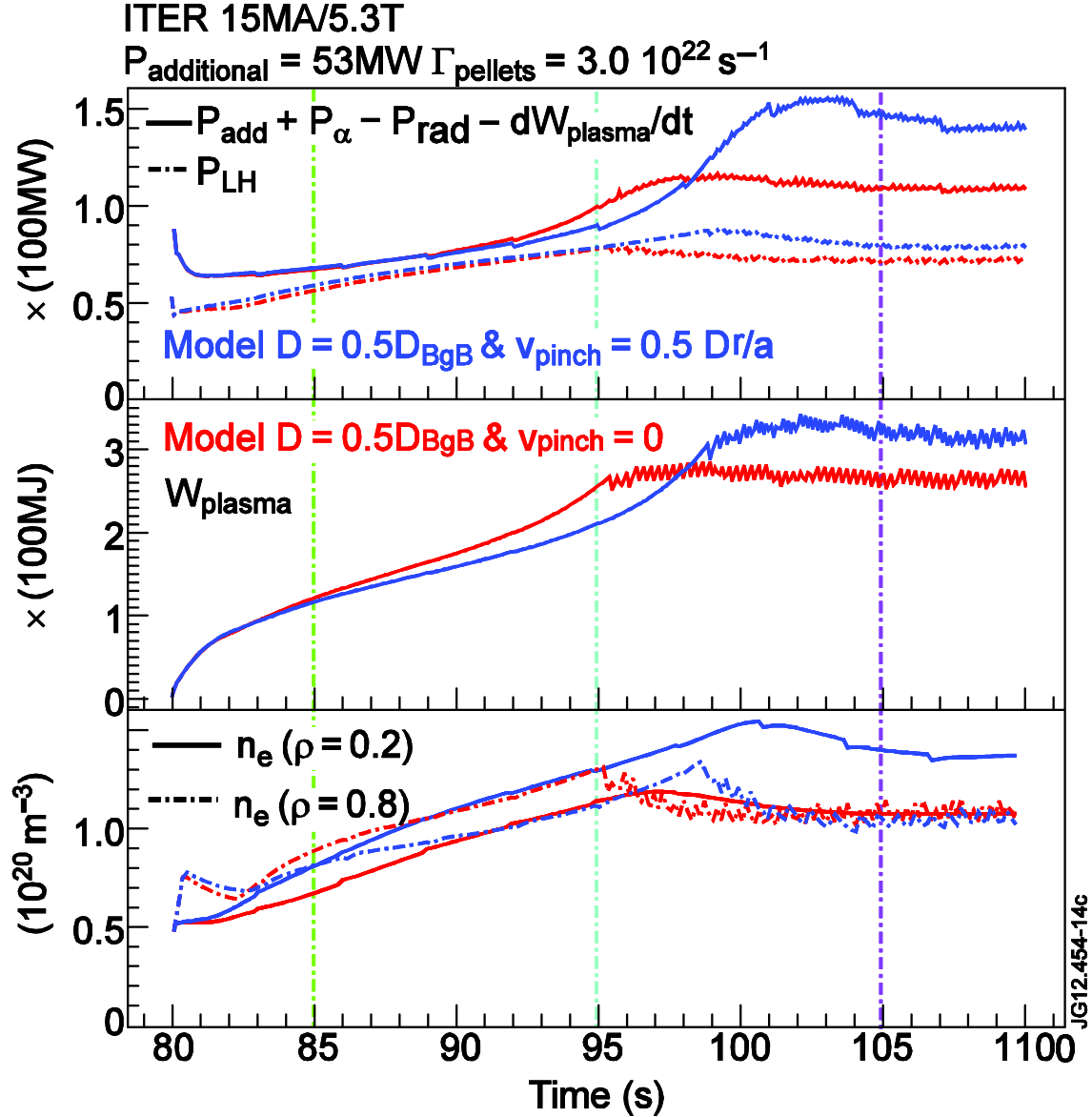


Figure 14. Simulation of access to burning plasma conditions in ITER with the two particle transport assumptions used to model JET high I_p H-modes illustrating the effect of the low diffusion coefficient during this phase and the effect of an additional particle pinch. Top) time evolution of the edge power flow and L-H transition power with the two particle transport assumptions. Middle) time evolution of the plasma thermal energy with the two particle transport assumptions. Bottom) time evolution of the core ($\rho=0.2$) and edge ($\rho=0.8$) plasma density with the two particle transport assumptions.

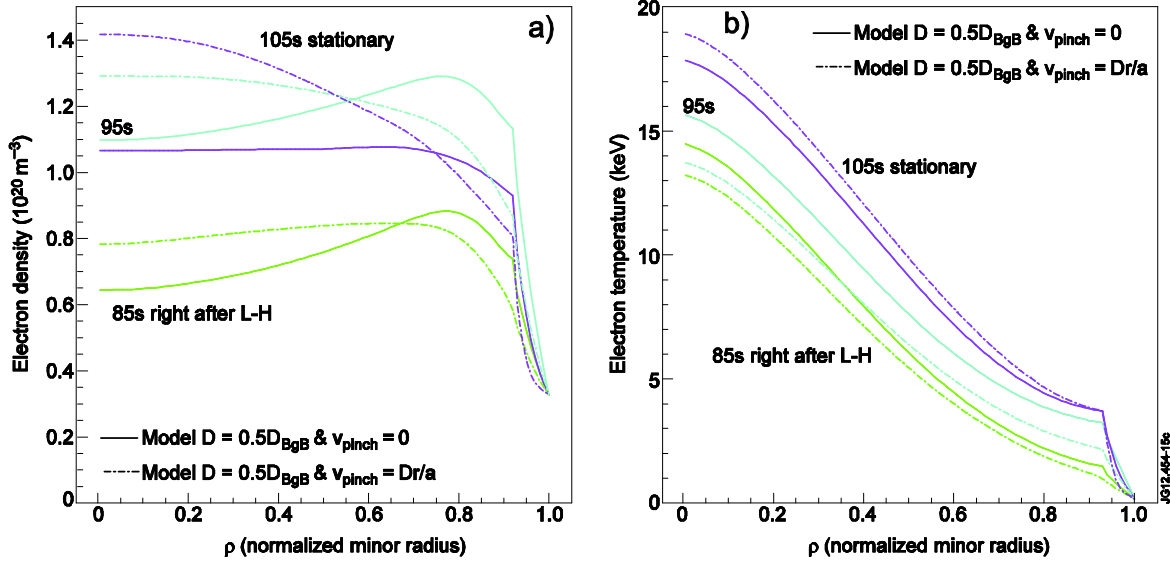


Figure 15. a) Electron density profiles at three times in the evolution towards burning plasma conditions in ITER Q_{DT} = 10 15 MA scenario with the two particle transport assumptions. b) Electron temperature profiles at three times in the evolution towards burning plasma conditions in ITER Q_{DT} = 10 15 MA scenario with the two particle transport assumptions.

5. Summary and Conclusions

In the present study we have analysed the build-up of plasma parameters following the H-mode transition in JET in view of its consequences for the alpha power evolution in the access to burning plasma conditions in ITER. The JET experiments show that the build-up of plasma temperature both at the plasma core and the plasma edge occurs in relatively short timescales, which are comparable to τ_E (energy confinement time of the stationary H-mode phases that follow the transient phases). On the contrary, the evolution of the edge and of the core density differ strongly depending on the level of plasma current in the discharge and the associated NBI penetration. For low plasma current H-modes (typically ≤ 2.5 MA for low δ discharges and ≤ 2.0 MA for high δ discharges) the edge and core density evolve in similar timescales to those of the edge and core plasma temperatures. For higher plasma current H-modes, the core density evolves in much longer timescales than the edge density leading to the formation of rather hollow density profiles, which persist for timescales of several τ_E until they are terminated by a sawtooth. The appearance of the hollow density profiles coincides with that of hollow NBI particle deposition profiles, which is associated with the density in the edge region of JET H-mode plasmas reaching a value of $\sim 6.5 \cdot 10^{19} \text{ m}^{-3}$. The long timescales for core density evolution in these conditions depend on the discharge plasma current and not on the value of the magnitude of the NBI particle deposition in the central region of the plasma.

Modelling of the density and temperature build-up after the H-mode transition in JET H-modes can reproduce the observed plasma behaviour if a purely-diffusive plasma behaviour is assumed for this transient phase (i.e. no inwards pinch) even for plasma conditions with a very low collisionality (i.e. similar to that of the burning plasma in 15 MA Q_{DT} = 10 conditions in ITER). The value of the diffusion coefficient required to reproduce the experiment has a value proportional (typically $\sim 1/4$ - $1/2$) to that of the usual values from the Bohm/GyroBohm model

used for the modelling of density profiles for stationary discharges at JET [Garzotti 2003]. This is unlike the assumptions required to model the stationary density profiles at JET which require a sizeable inwards pinch velocity, in agreement with expectations from turbulent particle transport [Angioni 2007a]. This difference indicates that the shape of the plasma density profile itself (i.e. the positive gradients in the radial direction for hollow profiles) may influence the ratio of the turbulent outwards versus inwards transport.

The same models and modelling assumptions as those applied to JET have been used to model the access to burning plasma conditions in ITER. The results obtained indicate that there is not a problem of edge power flow in the access to $Q_{DT}=10$ in ITER if core particle transport behaves diffusively during this phase. That is, the edge power does not undershoot by a significant amount and length of time the H-mode power threshold in the access to burning plasma conditions after the H-mode transition. This is due to the slow rise of the core plasma density which leads to the formation of hollow density profiles and allows the core temperature and the alpha heating power to increase monotonically in time after the H-mode transition. If a particle pinch is assumed, with values similar to those which overestimate but are not grossly in contradiction with the JET experimental results, hollow density profiles are not formed after the H-mode transition. This leads to a lower increase of the core plasma temperature after the H-mode transition than for the purely-diffusive case. Even in this case the alpha power is sufficient to maintain the edge power flow above the H-mode threshold power during this case. However, in this case the phase during which the edge power flow remains close to the H-mode threshold power is longer than for the purely diffusive case, which increases the likelihood of a H-L back transition during that phase.

While the results and extrapolation of the JET plasma behaviour to ITER are very encouraging, there remain uncertainties to be resolved associated with the different heating methods used in JET and ITER and its possible influence on turbulent particle transport. In the JET plasmas considered in this study, the power is mainly deposited in the ions and then transferred to the electrons by equipartition. The ITER plasmas will be dominantly electron heated with the ions being heated predominantly by equipartition from the electrons. In addition, the power deposition profiles in ITER will be peaked near the plasma centre while the (NBI) power deposition profiles in JET are hollow for the ITER-relevant conditions analysed in this paper. This, in addition to the hollow density profiles themselves, can affect the temperature gradients in the plasma during the transient phases after the H-mode transition. The particle transport characteristics could thus be different between JET and ITER even when the plasma collisionality is the same. Progressing further in this area requires additional ITER/JET modelling and JET experiments. Modelling of turbulent particle transport for the phase after the H-mode transition at JET and for the access phase to burning plasma conditions in ITER with hollow density profiles should be carried out, ideally in an iterative way with transport codes, so that a complete physics-based modelling of this phase is developed. In addition, further experiments at high plasma current, in which sufficient central electron heating is provided to the JET plasmas while maintaining a low core particle source from NBI heating, should be carried out. This would allow determining experimentally if the low level of core heating (and, particularly, electron heating) plays an important role in the slow time scales for core density evolution in the transient phase after H-mode access of JET high current discharges.

Disclaimer: The views and opinions expressed herein do not necessarily reflect those of the European Commission or those of the ITER Organization or those of Fusion for Energy.

Acknowledgement: M. Maslov, C. Bourdelle, B. Baiocchi and C. Angioni are gratefully acknowledged for enlightening discussions on the physics of turbulent transport.

5. References

- [Angioni 2007a] Angioni, C., et al., Nucl. Fusion **47** (2007) 1326.
- [Angioni 2007b] Angioni, C., et al., Phys. Plasmas **14** (2007) 055905.
- [Angioni 2009] Angioni, C., et al., Nucl. Fusion **49** (2009) 055013.
- [Beurskens 2009] Beurskens, M.N.A., et al., Nucl. Fusion **49** (2009) 125006.
- [Beurskens 2013] Beurskens, M.N.A., et al., Nucl. Fusion **53** (2013) 013001.
- [Garzotti 2003] Garzotti, L., et al., Nucl. Fusion **43** (2003) 1829.
- [Garzotti 2012] Garzotti, L., et al., Nucl. Fusion **52** (2012) 013002.
- [Groebner 2001] Groebner R. J., et al., Nucl. Fusion **41** (2001) 1789.
- [Hawryluk 2009] Hawryluk, R.J., et al., Nucl. Fusion **49** (2009) 065012.
- [Hender 2007] Hender, T.C., et al., Nucl. Fusion **47** (2007) S128.
- [Loarte 2002] Loarte, A., et al., Plasma Phys. Control. Fusion **44** (2002) 1815.
- [Martin 2008] Martin, Y.R., et al., Journal of Physics: Conference Series **123** (2008) 012033.
- [Nunes 2010] Nunes, I., et al, Proc. 23rd IAEA Fusion Energy Conference Daejon, Republic of Korea, 2010, Paper EXC/8-4.
- [Pacher 2008] Pacher, G.W., et al., Nucl. Fusion **48** (2008) 105003.
- [Sartori 2004] Sartori, R., et al., Plasma Phys. Control. Fusion **46** (2004) 723.
- [Scotti 2012] Scotti, F., et al., 39th EPS Conference & 16th Int. Congress on Plasma Physics, Stockholm, paper. P4.031.
- [Wagner 2010] Wagner, F., et al., Plasma Phys. Control. Fusion **52** (2010) 124044.